ACS OMEGA

http://pubs.acs.org/journal/acsodf

Article

Sensitive Electrochemical Sensor Based On an Aminated MIL-101(Cr) MOF for the Detection of Tartrazine

Raïssa Tagueu Massah, Sherman Lesly Zambou Jiokeng, Jun Liang, Evangeline Njanja, Tobie Matemb Ma Ntep, Alex Spiess, Lars Rademacher, Christoph Janiak, and Ignas Kenfack Tonle*

Cite This: *ACS Omega* 2022, 7, 19420−19427

Read Online

ACCESS | Metrics & More | Article Recommendations | Supporting Information

ABSTRACT: The aminated metal−organic framework H_2N-MIL-101(Cr) was used as the carbon paste electrode (CPE) modifier for the determination of tartrazine (Tz) in soft drinks. The amino material was characterized by electrochemical impedance spectroscopy and showed significantly faster electron transfer with lower charge-transfer resistance (0.13 kΩ) compared to the electrode modified with the unfunctionalized MIL-101(Cr) material (1.1 kΩ). The H_2N-MIL-101(Cr)-modified CPE [H_2N-MIL-101(Cr)-CPE] was then characterized by cyclic voltammetry (CV) using $[Fe(CN)_6]^{3-}$ and $[Ru(NH_3)_6]^{3+}$ ions as the redox probes, showing good accumulation of $[Fe(CN)_6]^{3-}$ ions on the electrode surface. A CV scan of Tz in Britton Robinson buffer solution revealed an irreversible system with an oxidation peak at +0.998 V versus Ag/AgCl/KCl. Using CV and differential pulse voltammetry, an electrochemical method for quantifying Tz in aqueous medium was then developed. Several parameters that affect the accumulation and detection steps were optimized. Optimal detection of Tz was achieved after 180 s of accumulation in Britton Robinson buffer solution (pH 2) using 2 mg of H_2N-MIL-101(Cr) material. Under optimal conditions, the sensor exhibited a linear response in the concentration range of 0.004−0.1 μM and good detection sensitivity (35.4 μA μM^{-1}), and the detection limit for Tz was found to be 1.77 nM (S/N = 3). Satisfactory repeatability, stability, and anti-interference performance were also achieved on H_2N-MIL-101(Cr)-CPE. The sensor was applied to commercial juices, and the results obtained were approximately similar to those given by UV−vis spectrophotometry.

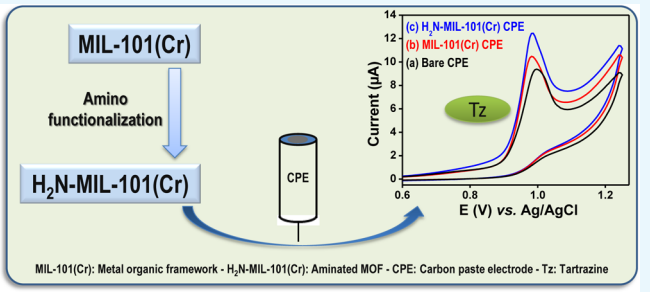

INTRODUCTION

Natural or synthetic dyes are often added to food and beverages to improve the appearance, flavor, texture, nutritional value, and shelf life of manufactured products.[1] Compared to natural dyes, synthetic food dyes have seen widespread use because of their low cost as well as higher stability to light, heat, and pH variations. One of the most common synthetic azo dyes used in foodstuffs and drinks is tartrazine (Tz) ($C_{16}H_9N_4Na_3O_9S_2$, referred hereafter as Tz), a lemon yellow colored dye also known as E102 in the food industry.[2] Unfortunately, excessive ingestion of Tz is associated (although controversial) with potential health issues including allergies, asthma, chronic hives, and hyperactivity in children.[3] The recommended acceptable intake of Tz is 7.5 mg/kg body weight per day, and the maximum Tz content of 150 μg/g in milk-based desserts, 200 μg/g in candied fruits and vegetables, and 100 μg/mL are permissible in soft drinks as prescribed by international organizations.[4] In view of risks associated with its abusive consumption, various methods have been developed for the determination of Tz, including chromatographic methods,[2,5,6] spectrophotometry,[7,8] and capillary electrophoresis.[9,10] Due to their excellent sensitivity, short analysis time, low energy consumption, and inexpensive equipment, electrochemical techniques are also increasingly being used and show promising applications in food safety analysis.[11] Various types of electrochemical sensors that have already been developed include sensors based on zinc oxide nanoparticles,[12] gold nanoparticles,[13] graphitic carbon nitride,[14] and carbon nanotubes.[15] More recently, sensors based on metal−organic frameworks (MOFs) have been introduced, taking advantage of the resultant increased electrode surface area and mass transport, as well as rapid electron transfer.[16,17]

MOFs are crystalline porous hybrid materials, consisting of metal cluster nodes which are bridged by polytopic organic ligands. Owing to the tunability of their structure as well as their pore surface chemistry via a linker or metal-cluster functionalization, MOFs show promising applications in many fields. These applications include gas storage, capture and separation; catalysis; heat transformation; and electroanaly-

Received: February 24, 2022
Accepted: May 12, 2022
Published: June 1, 2022

sis.[18] In particular, the chromium(III) terephthalate MOF denoted as MIL-101(Cr) has previously been reported as an excellent electrode material for the detection of analytes like ascorbic acid (AA) and sulfites.[19] In addition to its huge surface area (up to 4000 $m^2\ g^{-1}$), presence of coordinatively unsaturated Cr sites (CUS), and hydrothermal and chemical stability, MIL-101(Cr) features a mesoporous structure to accommodate large-sized/bulky analytes like Tz.[20,21] Moreover, functionalization of its framework with an organic group like the amino group could further improve the sensitivity and/or selectivity of the electrode. Amino functionalization of MOFs was demonstrated to improve adsorptive properties toward the uptake of target molecules such as methyl orange,[22] *p*-nitrophenol,[23] and CO_2[24−26]

Herein, we report the electrochemical detection of Tz using a carbon paste electrode (CPE) modified with the amino-functionalized MOF H_2N-MIL-101(Cr). The electrode response was compared with the signals recorded on the bare CPE and H_2N-MIL-101(Cr)-CPE in order to highlight the specific input of amino functional groups in the detection of Tz. The obtained H_2N-MIL-101(Cr)-CPE electrode was optimized and then successfully applied for the determination of Tz in commercial soft drink samples.

RESULTS AND DISCUSSION

Synthesis and Characterizations. Upon synthesis, the aminated MOF was structurally characterized by X-ray diffraction (XRD), IR spectroscopy, and N_2 sorption experiments [Brunauer−Emmett−Teller (BET) method]. As shown by Figure S1 (Supporting Information), its powdered pattern matched well with the simulated MIL-101(Cr) curve, characterized by a well-established crystallinity, which is usual for this mesoporous material.[24,25] The diffraction peaks and the XRD pattern of NH_2-MIL-101(Cr) were in good agreement with those reported previously,[26,27] indicating the successful synthesis of NH_2-MIL-101(Cr).

As shown by Figure 1a, the Fourier transform infrared (FT-IR) spectra of H_2N-MIL-101(Cr) and MIL-101(Cr) materials exhibited similar absorption bands in the range 1500−400 cm^{-1}; while additional bands appeared between 3200 and 3500 cm^{-1}, at 1621 and 1340 cm^{-1} for H_2N-MIL-101(Cr). The double bands at 3490 and 3383 cm^{-1} were assigned to the asymmetric and symmetric stretching vibrations of $-NH_2$, while the bands at 1621 and 1340 cm^{-1} were attributed to the N−H bending vibration and C_{Arom}−N stretching, respectively. This is consistent with the amino functionalization of H_2N-MIL-101(Cr) with respect to unmodified MIL-101(Cr) as also reported in other works.[3,28]

Nitrogen sorption experiments conducted on MIL-101(Cr) and H_2N-MIL-101(Cr) at 77 K yielded type Ib isotherms[29] for both materials (Figure 1b), which is due to the presence of micropores in both MOFs. The nitrogen uptake in H_2N-MIL-101(Cr) was significantly smaller compared to that in MIL-101(Cr), resulting in a BET surface area of 1175 $m^2\ g^{-1}$ [3100 $m^2\ g^{-1}$ for MIL-101(Cr)] and pore volume of 0.65 $cm^3\ g^{-1}$ [1.5 $cm^3\ g^{-1}$ for MIL-101(Cr)]. The decrease in the specific surface area and pore volume in H_2N-MIL-101(Cr) material was attributed to the steric occupation of the pores by $-NH_2$ groups. All data obtained for the comparative characterization of MIL-101(Cr) and H_2N-MIL-101(Cr) indicated the successful modification by grafting of the pristine MOF.

Electrochemical and Morphologic Characterization of Modified Electrodes. Multisweep cyclic voltammetry was applied to investigate the charge selectivity properties of the MIL-101(Cr) MOFs before and after its modification. Thus, unmodified CPE, MIL-101(Cr)-CPE, and H_2N-MIL-101(Cr)-CPE were prepared and tested in 0.1 M KCl (at pH 2) toward the accumulation of $[Fe(CN)_6]^{3-}$ and $[Ru(NH_3)_6]^{3+}$ electroactive probes, as shown in Figure 2.

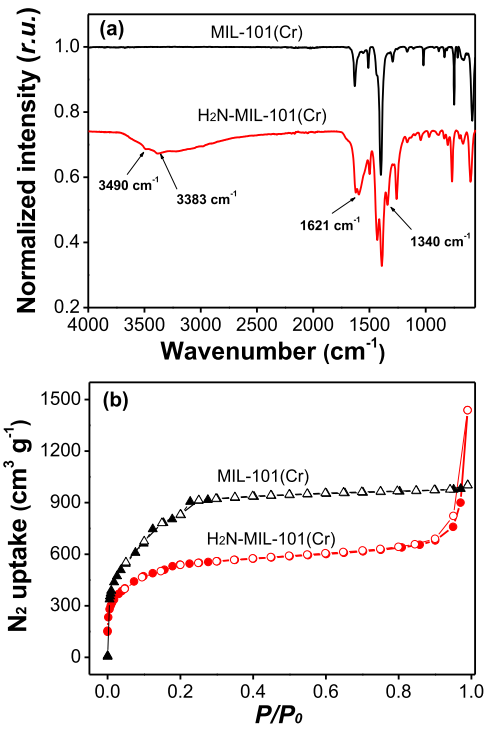

Figure 1. (a) FT-IR spectra and (b) N_2 adsorption−desorption isotherms of MIL-101(Cr) and H_2N-MIL-101(Cr).

One can observe in Figure 2a that, by continuously cycling, $[Fe(CN)_6]^{3-}$ ions were progressively accumulated on H_2N-MIL-101(Cr)-CPE as the anodic (I_a) and cathodic (I_c) currents increased between cycles. Upon saturation, the anodic and cathodic peak currents recorded on H_2N-MIL-101(Cr)-CPE were 260.1 and 259.5 μA, respectively. These values were greater than those measured on MIL-101(Cr)-CPE (Ia = 132.9 μA and Ic = 115.9 μA) and on bare CPE (Ia = 89.7 μA and Ic = 89.6 μA) (Figure 2b). This difference was explained by the electrostatic attraction between the protonated NH_3^+ groups on H_2N-MIL-101(Cr) and the negatively charged $[Fe(CN)_6]^{3-}$ ions. By replacing $[Fe(CN)_6]^{3-}$ by $[Ru(NH_3)_6]^{3+}$ ions, performing the same experiment (Figure S2a, Supporting Information) yielded stable voltammograms with peak current values of 34.5 μA (Ia) and 46.2 μA (Ic), suggesting no uptake of the cationic probe. Even on MIL-101(Cr)-CPE, similar results were obtained (Figure S2b, Supporting Information). This behavior (non-accumulation) was ascribed to the repulsion between $[Ru(NH_3)_6]^{3+}$ ions and protonated amine groups on H_2N-MIL-101(Cr), as described by previous works performed using aminated clay minerals.[30] These results clearly show that H_2N-MIL-101(Cr) materials could be applied as an electrode material for the electrochemical detection of anionic compounds. It was further used to build a sensor for analysis of Tz.

The morphology of the CPE before and after its modification in turn by MIL-101(Cr) and H_2N-MIL-101(Cr) was studied by scanning and transmission electron microscopy (STEM) combined with energy-dispersive X-ray

https://doi.org/10.1021/acsomega.2c01106
ACS Omega 2022, 7, 19420−19427

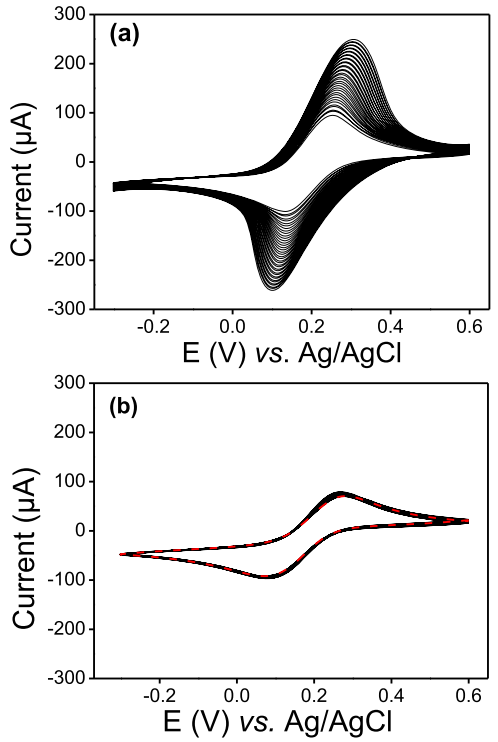

Figure 2. Multisweep cyclic voltammograms recorded at 50 mV s^{-1} in 0.1 M KCl solution containing 1 mM $[Fe(CN)_6]^{3-}$ using H_2N-MIL-101(Cr)-CPE (a) and MIL-101(Cr)-CPE (b). The dot red line in b corresponds to the bare CPE.

spectroscopy (EDX). As shown by Figure S3 (Supporting Information) and EDX data, the STEM image for the unmodified CPE was very bright due to the high amount of carbon (96.77 %At by EDX). The STEM−EDX of MIL-101(Cr)-CPE showed mainly the presence of carbon (particles with less contrast) and chrome, while H_2N-MIL-101(Cr)-CPE showed agglomerated nanoparticles, probably Cr-NPs as compared with powder X-ray diffraction results.

The active surface areas of all the prepared working electrodes were evaluated by analyzing the cyclovoltammograms of these electrodes, recorded in 0.1 M KCl + 1 mM $[Fe(CN)_6]^{3-}$, while the potential scan rate (v) was varied from 10 to 120 mV s^{-1}. The peak currents (Ip) in both anodic and cathodic directions increased proportionally with $v^{1/2}$ (see Figure S4, Supporting Information), indicating that the redox process on these electrodes is diffusion controlled. By exploiting the Randles−Sevcik equation, the slopes of Ip versus $v^{1/2}$ plots and the diffusion coefficient (D) value for $[Fe(CN)_6]^{3-}$ (7.6×10^{-6} cm^2 s^{-1}),[31] the electroactive surface areas of 0.031, 0.220, and 0.086 cm^2 were calculated for CPE, MIL-101(Cr)-CPE, and H_2N-MIL-101(Cr)-CPE, respectively. Overall, the obtained values indicated that MIL-101(Cr) displayed electroactive surface areas 7.1-fold and 2.6-fold higher than those of bare CPE and H_2N-MIL-101(Cr)-CPE, respectively.

Electrochemical impedance spectroscopy was also used to assess the electron-transfer rate of CPE, MIL-101(Cr)-CPE, and H_2N-MIL-101(Cr)-CPE using the $[Fe(CN)_6]^{3-/4-}$ redox couple. The corresponding obtained Nyquist diagrams are shown in Figure 3. A charge-transfer resistance (R_{CT}) of 7.8 kΩ was recorded for the bare CPE (Figure 3a). Upon modification using MIL-101(Cr) MOFs, the R_{CT} decreased to 1.1 kΩ

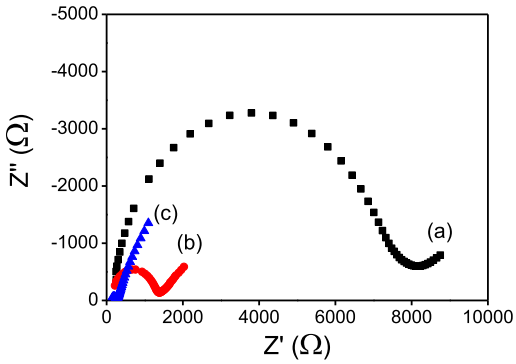

Figure 3. Nyquist diagrams recorded in 0.1 M KCl containing 1 mM $[Fe(CN)_6]^{3-/4-}$ on CPE (a), MIL-101(Cr)-CPE (b), and H_2N-MIL-101(Cr)-CPE (c).

(Figure 3b) and further to 0.13 kΩ on the H_2N-MIL-101(Cr)-CPE (Figure 3c).

These data pointed out a process limited by electron transfer. Overall, the modification of the CPE with H_2N-MIL-101(Cr) led to a higher electron-transfer capacity. The sensitivity of this sensor was further tested toward the electrochemical behavior of Tz.

Electrochemical Behavior of Tz and Effect of Detection Medium. The redox behavior of Tz, investigated by CV on all prepared electrodes is shown on Figure 4. On

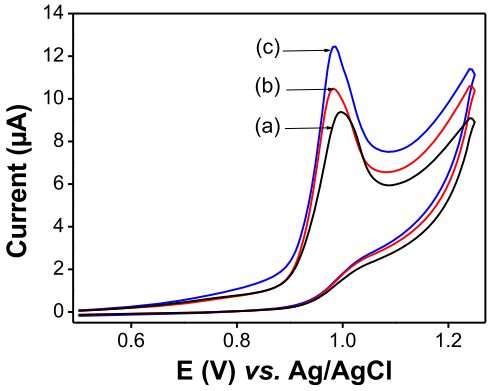

Figure 4. Cyclic voltammograms recorded at 50 mV s^{-1} for 0.4 mM Tz solution in 0.1 M ABS (pH 4) at (a) CPE, (b) MIL-101(Cr)-CPE, and (c) H_2N-MIL-101(Cr)-CPE.

these electrodes, Tz exhibited an irreversible anodic peak around +0.998 V. The peak intensity (12.40 μA) obtained on the H_2N-MIL-101(Cr)-CPE (Figure 4a) was 1.19 and 1.40-fold greater than those obtained on MIL-101(Cr)-CPE (I_{pa} = 10.46 μA, Figure 4b) and CPE (I_{pa} = 9.19 μA, Figure 4c). As explained in the previous section, this result was assigned to favorable electrostatic attractions between Tz and ^+H_3N-MIL-101(Cr) materials. The obtained result indicated that H_2N-MIL-101(Cr) has improved the electro-oxidation of Tz. Because the detection medium usually plays an important role in the sensitivity of each electrochemical method, the effect of the nature of detection solution was investigated.

Thus, three media at the same concentration were tested: phosphate buffer, Britton Robinson buffer, and acetate buffer solutions, in the presence of 0.4 mM Tz. Figure S5 (Supporting Information) shows a CV of 0.4 mM Tz on H_2N-MIL-101(Cr)-CPE in these three media at pH 4. The

https://doi.org/10.1021/acsomega.2c01106
ACS Omega 2022, 7, 19420−19427

results show a better anodic peak current with Britton Robinson buffer solution, which was chosen as the detection medium for subsequent experiments.

Effect of Potential Scan Rate. In order to identify the transport process of the analyte at the surface of H_2N-MIL-101(Cr)-CPE, the influence of the potential scan rate on the electrochemical response of Tz was studied by CV. As can be seen in Figure 5, the anodic peak current (I_a) increased with

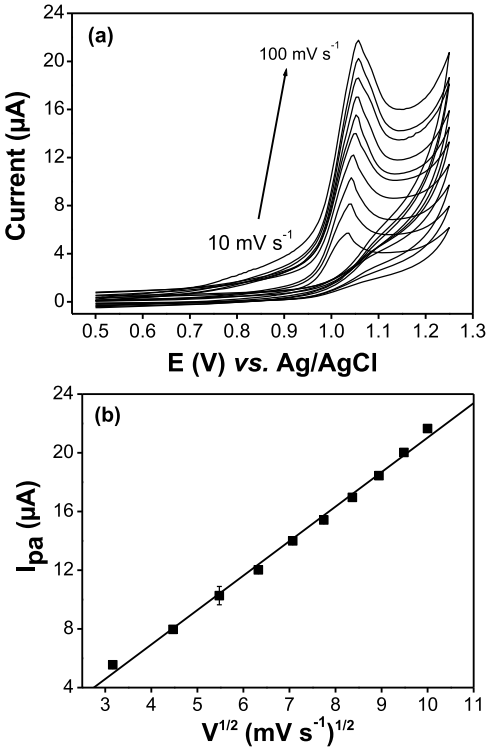

Figure 5. (a) Cyclic voltammograms recorded for 0.4 mM Tz in 0.1 M BRBS (pH 2) on H_2N-MIL-101(Cr)-CPE at different scan rates (10−100 mV s^{-1}) and (b) peak current as a function of $v^{1/2}$.

the scan rates (v) in the studied range (10−100 mV s^{-1}) (Figure 5a), while a linear dependence was observed between $v^{1/2}$ and I_a (Figure 5b), expressed by eq 1

$$I_a = 2.349\, v^{1/2} - 2.461 (R^2 = 0.996) \quad (1)$$

This indicated a diffusion-controlled process that was also confirmed by plotting the double logarithm of I_a versus v (see Figure S6a, Supporting Information) characterized by a slope of 0.59 greater than the expected 0.5, the indicative and significant value for a diffusion-controlled electron-transfer mechanism.[32] One can conclude that the electro-oxidation of Tz is a mixture of absorption and diffusion-controlled processes with diffusion predominating. Also, the presence of a non-zero intercept point (−2.461) on the y-axis (I_a vs $v^{1/2}$) indicated and confirmed the presence of some adsorption process associated with the diffusion-controlled electron-transfer mechanism. With the increase of scan rate, the oxidation peak potentials (E_a) moved to the positive direction. The peak potential (E_p) was linearly proportional to log.v (Figure S6b, Supporting Information), according to eq 2

$$E_p = 1.08 + 0.026 \log v (R = 0.983) \quad (2)$$

Confronting eq 2 with the Laviron's eq 3 for an irreversible electrode process[33] allowed to obtain some kinetics parameters such as α (transfer coefficient) and the standard rate constant of the reaction k^0 (cm s^{-1}).

$$E_p = E^0 + \left(\frac{2.303\, RT}{\alpha nF}\right)\log\left(\frac{RTk^0}{\alpha nF}\right) + \left(\frac{2.303\, RT}{\alpha nF}\right)\log v \quad (3)$$

n is the number of electrons transferred, v is the scan rate, and E^0 is the formal redox potential. From the slope of E_p vs log$v$, αn was calculated to be 2.31.

Bard and Faulkner equation: $\alpha = 47.7/(E_p - Ep/2)$ was used for the calculation of α.[33,34] From the above-mentioned equation, $\alpha = 1.4$, while the number of electrons transferred was 1.65 ≈ 2.

Effect of the Amount of H_2N-MIL-101(Cr) in the CPE. The optimal mass of H_2N-MIL-101(Cr) within the CPE is a key data for the best response of the sensor. Hence, several H_2N-MIL-101(Cr)-CPEs were prepared, containing 0, 1, 2, 3, 4, and 5 mg of MIL-101(Cr)−NH_2, corresponding to 0, 2, 4, 6, 8, and 10% wt MIL-101(Cr)−NH_2. Afterward, they were tested for the determination of Tz. As shown in Figure 6, there was a

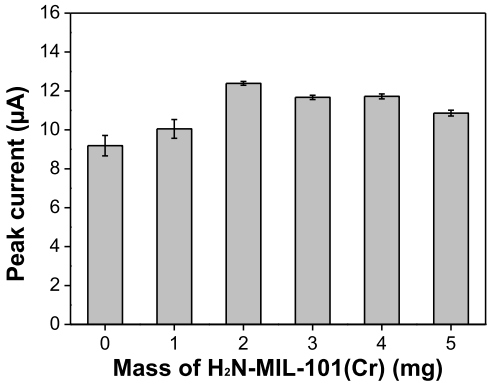

Figure 6. Effect of the amount of H_2N-MIL-101(Cr) (in mg) on the CV peak current of 0.4 mM Tz in 0.1 M BRBS (pH 4) on H_2N-MIL-101(Cr)-CPE. Experiments were performed in triplicate.

significant increase in peak current up to 2 mg of H_2N-MIL-101(Cr), followed by a slight decrease in the electrode response as the amount of H_2N-MIL-101(Cr) increased. The increase in peak current was probably due to the augmentation of binding sites on the electrode surface, available to bind more Tz molecules. The decrease in peak current observed above 2 mg was obviously due to the decrease in the conductivity of the electrode. For further experiments, the percentage of H_2N-MIL-101(Cr) in the CPE was kept at 4% wt.

Effect of pH on the Peak Current and Potential. To select the suitable pH value for Tz electrochemical determination, the pH of Britton Robinson buffer solution employed as a detection medium was varied between 2 and 9 (Figure 7). It was observed that the signal of Tz oxidation is highly dependent on the acidity of the supporting electrolyte (Figure 7a). The best electrode signal was obtained at pH 2, while the electro-oxidation of Tz became less significant with an increase in pH as protons are directly involved in the redox reaction at a H_2N-MIL-101(Cr) sensor. Moreover, the peak potential of Tz shifted toward more negative values with the increase in pH [curve (ii), Figure 7b] in accordance with the following equation: $E_p = 1.454 - 0.03$ pH ($R^2 = 0.997$). The value of the

https://doi.org/10.1021/acsomega.2c01106
ACS Omega 2022, 7, 19420−19427

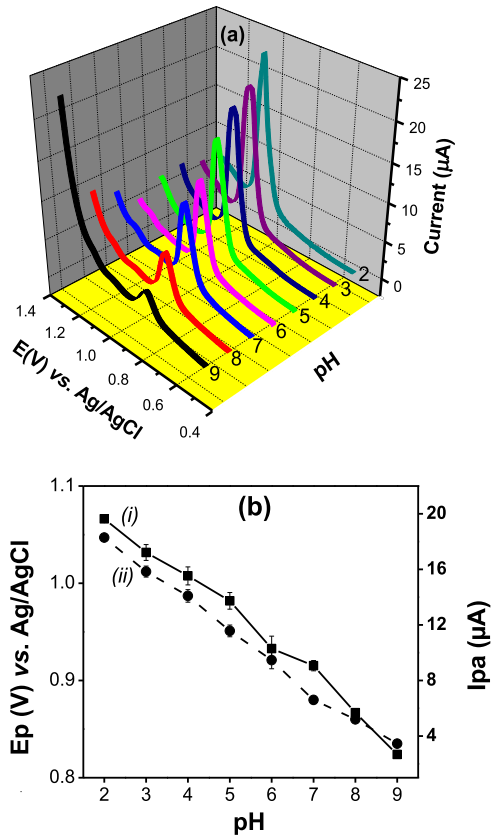

Figure 7. (a) Effect of the pH of the detection medium on the electrochemical response of 0.02 mM Tz-in BRBS on H_2N-MIL-101(Cr)-CPE and (b) plot of I_a versus pH (i) and peak potential (E_p) versus pH (ii).

slope (−0.03 V/pH) not close to the theoretical Nernstian value of (−0.059 V/pH) suggested that the number of electrons involved in the oxidation of Tz is different from the number of protons. Clearly, it appeared that two electrons and one proton are involved in the oxidation of Tz, as proposed in Scheme 1. As the pH of the supporting electrolyte increased, the anodic peak current of Tz decreased [Figure 7b see curve (i)]. Interestingly, the peak current rose to the maximum value (19.63 μA) at pH 2. It is known that Tz presents two strong sulfonic acid groups (pK_a = 2), one acetate weak acid group (pK_a = 5), and one azo group (pK_a = 10.86).[35]

From pH 2−5, the azo group is protonated and the two strong sulfonic acid groups are deprotonated, a charge of Tz is 1^-. After pH 5 (and up to 9), the charge is 2^- with deprotonation of acetate acid group and the molecule is highly hydrophilic.

In acidic media, the oxidation process is facilitated due to easy protonation of the azo group resulting in the decreased electron density and thus in the increased voltammetric signal. On the other hand, the highly improved voltammetric signal over aminated MIL-101(Cr) could be explained similarly, together with a possible ion−dipole interaction between the $-SO_3^-$ anionic group of Tz and the $-NH_3^+$ protonated function of H_2N-MIL-101(Cr).

At higher pH values, the net charge is increased (1^- to 2^-) and Tz is not adsorbed on the electrode surface, due to the electrostatic repulsion between the deprotonated two sulfonic acid ($-SO_3^-$), one acetate acid ($-COO^-$) group present on

Scheme 1. Proposed Electrochemical Reaction of Tz at H_2N-MIL-101(Cr)-CPE

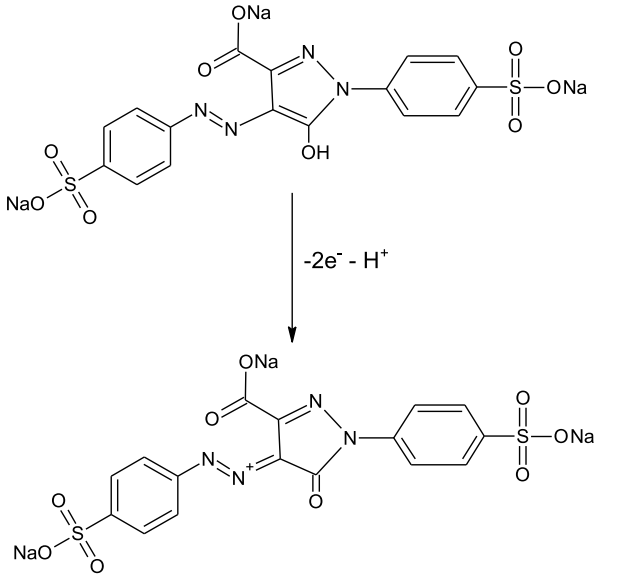

Tz, and electron pairs of oxygen in the hydroxy of terephthalic acid.

Because 0.1 M BRBS (pH 2) was the optimum pH, this medium was used in all further experiments.

Effect of the Accumulation Time. Accumulation time is another useful parameter in electrochemical analysis. It was investigated and Figure 8 shows a rapid response of the

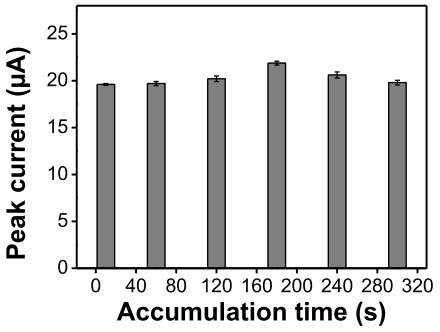

Figure 8. Effect of the accumulation time on the electrochemical response of 0.02 mM Tz $^-$in BRBS (pH 2) on H_2N-MIL-101(Cr)-CPE. Experiments were performed in triplicate.

electrode with a peak current of 19.6 μA after 10 s of accumulation. Afterward, the peak intensity was stabilized due to saturation of the fixation sites on the electrode surface. 180 s was therefore chosen as the optimal time for further investigation.

Calibration Curve. Keeping the optimized experimental conditions, differential pulse voltammetry (DPV) was performed to establish the relationship between the peak current and the concentration of Tz at H_2N-MIL-101(Cr)-CPE. Figure 9 shows the corresponding i-E curves: the oxidation peak current increased with increasing concentration of Tz in the range of 0.004 to 0.1 μM. The plot of anodic peak current as a function of Tz concentration was linear, as shown by the inset in Figure 9. The calibration curve followed the equation I_{pa} (μA) = 0.908 + 35.4[Tz] (μM), with a correlation coefficient of 0.999. A sensitivity of 35.4 μA μM^{-1} obtained

https://doi.org/10.1021/acsomega.2c01106
ACS Omega 2022, 7, 19420−19427

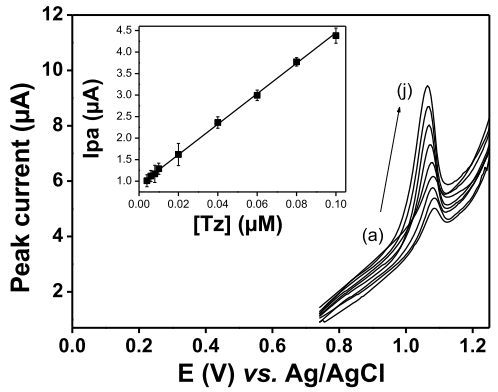

Figure 9. DPV responses recorded on H_2N-MIL-101(Cr)-CPE in 0.1 M BRBS (pH 2) containing Tz at different concentrations: (a−i): 0.004−0.1 μM. Inset shows the corresponding calibration graph. Experiments were performed in triplicate.

reflects the change in the response of a sensor to a small change in stimulus causing the response and corresponds to the slope of the calibration curve.[36] The limit of detection (LOD) corresponds to the lowest concentration of an analyte that can be detected.[37] Based on a signal-to-noise ratio of 3, a LOD of 1.77 nM was obtained using the equation LOD = 3 S/m, where S is the standard deviation of blank and m is the slope of the regression line. The obtained LOD is one of the lowest values reported for Tz detection (Table 1), which reveals that a H_2N-MIL-101(Cr)-CPE electrochemical sensor is sensitive for the determination of Tz.

Table 1. Comparison of the Performance of Some Tz Sensors Based on Modified Electrodes

electrode configuration	method	detection medium (pH)	detection limit (μM)	refs
gold nanoparticles/CPE	DPV	PBS (4.0)	0.002	13
[a]g-C_3N_4/graphite	DPV	PBS (2.1)	0.21	14
[b]MWCNTs/GCE	DPV	PBS (7.0)	0.22	35
[c]Gr/PLPA/PGE	DPV	PBS (7.0)	0.154	38
hemin/GCE	[d]SWV	PBS (7.4)	0.36	39
[e]MIP/GCE	SWV	PBS (7.0)	0.001	40
H_2N-MIL-101(Cr)-CPE	DPV	PRBS (2.0)	0.00177	this work

[a]g-C_3N_4: graphitic carbon nitride. [b]MWCNTs: multiwalled carbon nanotubes. [c]Gr/PLPA/PGE: graphene/poly(L-phenylalanine)/pencil graphite electrode. [d]SWV: square wave voltammetry. [e]MIP: molecularly imprinted polymer.

The stability and reproducibility of the proposed aminated MOF-modified electrode were also checked by measuring within days and for 5 successive days the signal (5 replicates) of 0.02 mM Tz in 0.1 M BRBS (pH 2.0). The voltammograms obtained (Figure S7, Supporting Information) evaluated the relative standard deviation at 3.5%, indicating an acceptable level of sensor reproducibility.

Interference Study and Analytical Application. The influence of potential interfering compounds such as AA, citric acid (CA), sodium benzoate, sodium sulfite, tartaric acid (TA), lactose, gallic acid (GA), curcumin (CUR), and butylated hydroxyanisole (BHA) at known concentrations (0.2, 2, 10, and 20 μM) on an oxidation peak current of 2 μM Tz in 0.1 M BRBS (pH 2) at H_2N-MIL-101(Cr)-CPE was examined. The results obtained are presented in Table 2. The tolerance limit was considered to be the concentration ratio of the additive to

Table 2. Tolerance Limits of Interfering Species in a Determination of 2 μM Tz

interfering species	tolerance limit ([additive]/[Tz])
AA	<1
CA	<0.5
TA	10
GA	<0.1
curcumin, Mg^{2+}, NO_3^-	0.1
BHA	1
lactose	5
sodium benzoate	<0.1
sodium sulfite, Ca^{2+}, Cl^-	10

Tz causing a relative error of less than 5.0%. The results in Table 2 show that the tolerance limits of Tz in the presence of 1-fold of BHA, 5-fold of lactose, and 10-fold of sodium sulfite, Ca^{2+}, and Cl^- were less than 5%, implying that the proposed modified electrode possessed excellent anti-interference ability and good selectivity.

Meanwhile, the oxidation peak of Tz was strongly affected by the presence of AA, CA, sodium benzoate, and GA. Thus, a sensor described herein is not advisable for media containing such compounds.

Finally, a H_2N-MIL-101(Cr)-CPE sensor was applied to the quality control of soft drinks from two different companies. The results obtained are presented in Table 3. For comparison

Table 3. Results of the Determination of Tz in Juice Samples

sample	H_2N-MIL-101(Cr)-CPE (mg L^{-1})	UV method (mg L^{-1})
juice 1	7.77 ± 1.57	7.50 ± 1.10
juice 2	5.93 ± 0.96	6.30 ± 1.10

purposes and to validate the developed electroanalytical method, Tz content of these samples was also determined by UV−vis spectrophotometry. In this experiment, the concentration of Tz was calculated using the standard addition method.

From the results obtained (Table 3), it can be noticed that the data from UV−vis spectrophotometry and voltammetric determinations are of the same order of magnitude, as the difference between the mean values is not significant.

According to European standards, the maximum amount of Tz present in soft drinks should be is 100 mg·L^{-1}. The results of these analyses, therefore, show the compliance with the standards by both companies. These results confirm the usefulness of the method and the sensor proposed herein.

CONCLUSIONS

In this work, a sensitive amperometric sensor based on the aminated H_2N-MIL-101(Cr)-modified CPE was proposed for the detection of Tz. The proposed sensor displayed great affinity toward the quantification of Tz, allowing its detection at the lowest concentration of 1.77 nM. Nevertheless, the H_2N-MIL-101(Cr)-CPE sensor showed interesting analytical performance, good stability, and reproducibility and may constitute an analytical tool of choice for the determination of Tz. Finally, MOF-modified electrodes could be used to create

https://doi.org/10.1021/acsomega.2c01106
ACS Omega 2022, 7, 19420−19427

smart devices for the sensing of biomolecules and other compounds, with a high level of reliability.

■ ASSOCIATED CONTENT

Supporting Information

The Supporting Information is available free of charge at https://pubs.acs.org/doi/10.1021/acsomega.2c01106.

Chemicals, materials, and procedures; synthesis of MIL-101(Cr) and H_2N-MIL-101(Cr); physico-chemical characterization; preparation of modified CPEs; electrochemical equipment and procedures; powder XRD analysis; STEM analyses; electrochemical characterization of modified electrodes using $[Ru(NH_3)_6]^{3+}$ ions; electroactive surface area determination; effect of detection medium; effect of potential scan rate; and reproducibility of H_2N-MIL-101(Cr)-CPE (PDF)

■ AUTHOR INFORMATION

Corresponding Author

Ignas Kenfack Tonle − *Electrochemistry and Chemistry of Materials, Department of Chemistry, University of Dschang, 00237 Dschang, Cameroon;* orcid.org/0000-0001-9794-788X; Email: ignas.tonle@univ-dschang.org

Authors

Raïssa Tagueu Massah − *Electrochemistry and Chemistry of Materials, Department of Chemistry, University of Dschang, 00237 Dschang, Cameroon*

Sherman Lesly Zambou Jiokeng − *Electrochemistry and Chemistry of Materials, Department of Chemistry, University of Dschang, 00237 Dschang, Cameroon*

Jun Liang − *Institut für Anorganische Chemie, Heinrich-Heine-Universität Düsseldorf, D-40204 Düsseldorf, Germany; Hoffmann Institute of Advanced Materials, Shenzhen Polytechnic, 518055 Shenzhen, China*

Evangeline Njanja − *Electrochemistry and Chemistry of Materials, Department of Chemistry, University of Dschang, 00237 Dschang, Cameroon*

Tobie Matemb Ma Ntep − *Institut für Anorganische Chemie, Heinrich-Heine-Universität Düsseldorf, D-40204 Düsseldorf, Germany*

Alex Spiess − *Institut für Anorganische Chemie, Heinrich-Heine-Universität Düsseldorf, D-40204 Düsseldorf, Germany*

Lars Rademacher − *Institut für Anorganische Chemie, Heinrich-Heine-Universität Düsseldorf, D-40204 Düsseldorf, Germany*

Christoph Janiak − *Institut für Anorganische Chemie, Heinrich-Heine-Universität Düsseldorf, D-40204 Düsseldorf, Germany*

Complete contact information is available at: https://pubs.acs.org/10.1021/acsomega.2c01106

Author Contributions

The manuscript was written through contributions of all authors, who have given approval to the final version of the manuscript.

Notes

The authors declare no competing financial interest.

■ ACKNOWLEDGMENTS

The authors gratefully acknowledge the support of the the Alexander von Humboldt Foundation (Germany).

■ REFERENCES

(1) Karim-Nezhad, G.; Khorablou, Z.; Zamani, M.; Dorraji, P. S.; Alamgholiloo, M. Voltammetric sensor for tartrazine determination in soft drinks using poly(p-aminobenzenesulfonic acid)/zinc oxide nanoparticle in carbon paste electrode. *J. Food Drug Anal.* **2017**, *25*, 293−301.

(2) Alves, S. P.; Brum, D. M.; de Andrade, É. C. B.; Netto, A. D. P. Determination of synthetic dyes in selected foodstuffs by high performance liquid chromatography with UV-DAD detection. *Food Chem.* **2008**, *107*, 489−496.

(3) Lin, Y.; Kong, C.; Chen, L. Direct synthesis of amine-functionalized MIL-101(Cr) nanoparticles and application for CO_2 capture. *RSC Adv.* **2012**, *2*, 6417−6419.

(4) FDA/CFSAN Food Advisory Committee, Center for Food. *Safety and Applied Nutrition, March 30−31*, Food Advisory Committee Meeting, 2011.

(5) Al-Degs, Y. S. Determination of three dyes in commercial soft drinks using HLA/GO and liquid chromatography. *Food Chem.* **2009**, *117*, 485−490.

(6) Culzoni, M. J.; Schenone, A. V.; Llamas, N. E.; Garrido, M.; Di Nezio, M. S.; Band, B. S. F.; Goicoechea, H. C.; Goicoechea, H. C. Fast chromatographic method for the determination of dyes in beverages by using high performance liquid chromatography-Diode array detection data and second order algorithms. *J. Chromatogr., A* **2009**, *1216*, 7063−7070.

(7) Capitán-Vallvey, L. F.; Iglesias, N. N.; de Orbe Payá, I.; Castaneda, R. A. Simultaneous determination of tartrazine and sunset yellow in cosmetic products by first-derivative spectrophotometry. *Microchim. Acta* **1997**, *126*, 153−157.

(8) Coelho, T. M.; Vidotti, E. C.; Rollemberg, M. C.; Medina, A. N.; Baesso, M. L.; Cella, N.; Bento, A. C. Photoacoustic spectroscopy as a tool for determination of food dyes: Comparison with first derivative spectrophotometry. *Talanta* **2010**, *81*, 202−207.

(9) Lee, K.-S.; Shiddiky, M. J. A.; Park, S.-H.; Park, D.-S.; Shim, Y.-B. Electrophoretic analysis of food dyes using miniaturized microfluidic system. *Electrophoresis* **2008**, *29*, 1910−1917.

(10) Ishikawa, F.; Oishi, M.; Kimura, K.; Yasui, A.; Saito, K. Determination of synthetic food dyes in food by capillary electrophoresis. *J. Food Hyg. Soc. Jpn.* **2004**, *45*, 150−155.

(11) Beitollahi, H.; Dourandish, Z.; Tajik, S.; Ganjali, M. R.; Norouzi, P.; Faridbod, F. Application of graphite screen printed electrode modified with dysprosium tungstate nanoparticles in voltammetric determination of epinephrine in the presence of acetylcholine. *J. Rare Earths* **2018**, *36*, 750−757.

(12) Karim-Nezhad, G.; Zeynab, K.; Maryam, Z.; Parisa, S. D.; Mahdieh, A. Voltammetric sensor for tartrazine determination in soft drinks using poly(p-aminobenzenesulfonic acid)/zinc oxide nanoparticle in carbon paste electrode. *J. Food Drug Anal.* **2016**, *25*, 293−301.

(13) Ghoreishi, S. M.; Behpour, M.; Golestaneh, M. Simultaneous determination of sunset yellow and tartrazine in soft drinks using gold nanoparticle carbon paste electrode. *Food Chem.* **2012**, *132*, 637−641.

(14) Karimi, M. A.; Aghaei, V. H.; Nezhadali, A.; Ajami, N. Graphitic carbon nitride as a new sensitive material for electrochemical determination of trace amounts of tartrazine in food samples. *Food Anal. Methods* **2018**, *11*, 2907−2915.

(15) Sierra-Rosales, P.; Toledo-Neira, C.; Squella, J. A. Electrochemical determination of food colorants in soft drinks using MWCNT-modified GCEs. *Sens. Actuators, B* **2017**, *240*, 1257−1264.

(16) Liu, L.; Zhou, Y.; Liu, S.; Xu, M. The application of metal-organic frameworks in electrochemical sensors. *Chemelectrochem* **2018**, *5*, 6−19.

(17) Pournara, A. D.; Tarlas, G. D.; Papaefstathiou, G. S.; Manos, M. J. Chemically modified electrodes with MOFs for the determination of inorganic and organic analytes via voltammetric techniques. A critical review. *Inorg. Chem. Front.* **2019**, *6*, 3440−3455.

(18) Janiak, C.; Vieth, J. K. MOFs, MILs and more: concepts, properties and applications for porous coordination networks (PCNs). *New J. Chem.* **2010**, *34*, 2366−2388.

(19) Massah, R. T.; Ma Ntep, T. J. M.; Njanja, E.; Jiokeng, S. L. Z.; Liang, J.; Janiak, C.; Tonle, I. K. A metal-organic framework-based amperometric sensor for the sensitive determination of sulfite ions in the presence of ascorbic acid. *Microchem. J.* **2021**, *169*, 106569.
(20) Férey, G.; Mellot-Draznieks, C.; Serre, C.; Millange, F.; Dutour, J.; Surblé, S.; Margiolaki, I. A chromium terephthalate-based solid with unusually large pore volumes and surface area. *Science* **2005**, *309*, 2040.
(21) Hong, D.-Y.; Hwang, Y. K.; Serre, C.; Férey, G.; Chang, J.-S. Porous chromium terephthalate MIL-101 with coordinatively unsaturated sites: surface functionalization, encapsulation, sorption and catalysis. *Adv. Funct. Mater.* **2009**, *19*, 1537−1552.
(22) Shuangyou, B.; Kai, L.; Ping, N.; Jinhui, P.; Xu, J.; Lihong, T. Synthesis of amino-functionalization magnetic multi-metal organic framework (Fe_3O_4/MIL-101($Al_{0.9}Fe_{0.1}$)/NH_2) for efficient removal ofmethyl orange from aqueous solution. *J. Taiwan Inst. Chem. Eng.* **2018**, *87*, 64−72.
(23) Lu, X.-t.; Pu, Y.-f.; Li, L.; Zhao, N.; Wang, F.; Xiao, F.-k.F. K. Preparation of metal-organic frameworks $Cu_3(BTC)_2$ with amino functionalization for CO_2 adsorption. *J. Fuel Chem. Technol.* **2019**, *47*, 338−343.
(24) Aldawsari, A. M.; Alsohaimi, I. H.; Hassan, M. A. H.; Berber, M. R.; Abdalla, Z. E. A.; Hassan, I.; Saleh, E. A. M.; Hameed, B. H. Activated carbon/MOFs composite: AC/NH_2-MIL-101(Cr), synthesis and application in high performance adsorption of p-nitrophenol. *J. Saudi Chem. Soc.* **2020**, *24*, 693−703.
(25) Lijuan, S.; Qi, K.; Wu, H.; Li, J.; Qiu, M.; Yi, Q. In-situ amino-functionalization of zeolitic imidazolate frameworks for high-efficiency capture of low-concentration CO_2 from flue gas. *Fuel* **2021**, *298*, 120875.
(26) Lin, Y.; Kong, C.; Chen, L. Direct synthesis of amine-functionalized MIL-101(Cr) nanoparticles and application for CO_2 capture. *RSC Adv.* **2012**, *2*, 6417−6419.
(27) Li, X.; Yunhong, P.; Qibin, X.; Zhong, L.; Jing, X. TiO_2 encapsulated in Salicylaldehyde-NH_2-MIL-101(Cr) for enhanced visible light-driven photodegradation of MB. *Appl. Catal., B* **2016**, *191*, 192−201.
(28) Jeremias, F.; Lozan, V.; Henninger, S. K.; Janiak, C. Programming MOFs for water sorption: amino-functionalized MIL-125 and UiO-66 for heat transformation and heat storage applications. *Dalton Trans.* **2013**, *42*, 15967−15973.
(29) Thommes, M.; Kaneko, K.; Neimark, A. V.; Olivier, J. P.; Rodriguez-Reinoso, F.; Rouquerol, J.; Sing, K. S. W. Physisorption of gases, with special reference to the evaluation of surface area and pore size distribution (IUPAC Technical Report). *Pure Appl. Chem.* **2015**, *87*, 1051−1069.
(30) Tchieno, F. M. M.; Sonfack, L. G.; Ymelé, E.; Ngameni, E.; Tonle, I. K. Electroanalytical application of amine-grafted attapulgite to the sensitive quantification of the bioactive compound mangiferin. *Electroanalysis* **2017**, *29*, 529−537.
(31) Chen, X.; Zhang, Y.; Li, C.; Li, C.; Zeng, T.; Wan, Q.; Li, Y.; Ke, Q.; Yang, N. Nanointerfaces of expanded graphite and Fe_2O_3 nanomaterials for electrochemical monitoring of multiple organic pollutants. *Electrochim. Acta* **2020**, *329*, 135118.
(32) Laviron, E. General expression of the linear potential sweep voltammogram in the case of diffusionless electrochemical systems. *J. Electroanal. Chem.* **1979**, *101*, 19−28.
(33) Bard, A. J.; Faulkner, L. R. *Electrochemical methods fundamentals and applications*, 2nd ed.; Wiley: New York, 2004; pp 286−293.
(34) Gómez, M.; Arancibia, V.; Rojas, C.; Nagles, E. Adsorptive stripping voltammetric determination of tartrazine and sunset yellow in gelatins and soft drink powder in the presence of cetylpyridinium bromide. *Int. J. Electrochem. Sci.* **2012**, *7*, 7493−7502.
(35) Sierra-Rosales, P.; Toledo-Neira, C.; Squella, J. A. Electrochemical determination of food colorants in soft drinks using MWCNT-modified GCEs. *Sens. Actuators, B* **2017**, *240*, 1257−1264.
(36) Pardue, H. L. Counterpoint the inseparable triad: analytical sensitivity, measurement uncertainty and quantitative resolution. *Clin. Chem.* **1997**, *43*, 1831−1837.
(37) Caucheteur, C.; Guo, T.; Albert, J. Review of plasmonic fiber optic biochemical sensors: improving the limit of detection. *Anal. Bioanal. Chem.* **2015**, *407*, 3883−3897.
(38) Tahtaisleyen, S.; Gorduk, O.; Sahin, Y. Electrochemical determination of tartrazine using a graphene/Poly(L-Phenylalanine) modified pencil graphite electrode. *Anal. Lett.* **2020**, *53*, 1683−1703.
(39) Sun, S.-C.; Hsieh, B.-C.; Chuang, M.-C. Electropolymerised-hemin-catalysed reduction and analysis of tartrazine and sunset yellow. *Electrochim. Acta* **2019**, *319*, 766−774.
(40) Jiang, S.; Xu, J.; Xu, P.; Liu, L.; Chen, Y.; Qiao, C.; Yang, S.; Sha, Z.; Zhang, J. A novel molecularly imprinted sensor for direct tartrazine detection. *Anal. Lett.* **2014**, *47*, 323−330.

https://doi.org/10.1021/acsomega.2c01106
ACS Omega 2022, 7, 19420−19427